



# Viscohydrodynamic lubrication in conformal contacts: A numerical approach

Michele Santeramo<sup>a</sup>, Giuseppe Carbone<sup>a,b</sup>, Georg Vorlaufer<sup>c</sup>, Stefan Krenn<sup>c</sup>,  
Carmine Putignano<sup>a,b,\*</sup>

<sup>a</sup> Department of Mechanics, Mathematics and Management, Politecnico di Bari, Via Orabona 4, 70100, Bari, Italy

<sup>b</sup> CNR Institute for Photonics and Nanotechnologies U.O.S. Bari, Physics Department M. Merlin, Via Amendola 173, I-70126, Bari, Italy

<sup>c</sup> AC2T research GmbH, Viktor-Kaplan-Straße 2/C, 2700 Wiener Neustadt, Austria

## ARTICLE INFO

### Keywords:

Journal bearing  
Soft matter  
Viscoelasticity  
Friction  
Lubrication

## ABSTRACT

The steady-state operation of a polymer journal bearing is investigated by means of an innovative numerical methodology, based on the definition of a viscoelastic Green's function intrinsically accounting for the circular hallmark of the contact domain. Crucially, results show, in terms of pressure, film thickness, and friction, the occurrence of a peculiar viscoelastohydrodynamic (VEHL) regime. This has critical consequences in applications, where the bearing capacity of the system may be affected. Ultimately, by focusing on different contact configurations, we show that the VEHL regime in polymer journal bearings is governed by three independent parameters, namely the Hersey number and the dimensionless velocities of the two interacting bodies.

## 1. Introduction

The importance that soft matter lubrication has gained in the industrial panorama is indubitable. This marked interest reflects the growing request for new polymers (Fusaro, 1990; Padovan et al., 1992; Yousef, 2016; Friedrich, 2018), biomedical implants (Askari and Andersen, 2018; Heß and Forsbach, 2021), and soft tissues (Heepe and Gorb, 2014). Indeed, these materials have a number of desirable qualities, including resistance to environmental conditions, light weights, and lower manufacturing costs. As a result, the continuous transition from metals to polymers in recent decades: seals (Dapp et al., 2012; Vlădescu et al., 2019), polymer bearings (Koike et al., 2012), and dampers (Shukla and Datta, 1999) are just examples. Nonetheless, because of their complex rheology, such materials' mechanical responses are sometimes difficult to predict: they display a significant time- and temperature-dependent behavior that can be characterized as viscoelastic. A clear understanding of the performance of this class of materials is indeed challenging, especially when other phases are involved as it occurs in lubricated contacts, but is of the utmost importance. Indeed, in spite of the considerable efforts in investigating dry contact mechanics involving soft materials (Hunter, 1961; Grosch, 1963; Persson, 2001; Carbone et al., 2009), limited research has been carried out to highlight the mechanisms governing the interactions at the lubricated interface in the presence of viscoelastic materials (Scaraggi and Persson, 2014; Putignano et al., 2016; Putignano, 2020; Putignano and Campanale, 2022). Furthermore, the presence of roughness may exacerbate even

more the complexity of the contact problem (Pandey et al., 2016; Venner and Lubrecht, 2000; Putignano et al., 2021). Pioneering studies were carried out by Rohde et al. (1979), who analyzed the effects of viscoelasticity and fluctuating loads on the elastohydrodynamic squeeze film, and by Elsharkawy (1996), who developed a numerical procedure to study the visco-elastohydrodynamic lubrication (VEHL) line contact problems based on an iterative Newton–Raphson scheme. Later, Hooke (1997) investigated the relationship between the lubrication behavior and dry contact pressures when soft solids are considered; in particular, in his analysis he found that the pressure distribution remains close to that obtained in dry, frictionless contact since the corresponding deformations are very large with respect to the film thickness. Another contribution has been provided by Scaraggi and Persson (2014), who examined the impact of random surface height fluctuations in lubricated contacts when linear viscoelastic solids are involved, and particular attention has been paid to the effects on the separation field and traction at the contact interfaces. Furthermore, Putignano and Dini (Putignano and Dini, 2017; Putignano, 2020; Putignano and Campanale, 2022) introduced a generalized numerical methodology for capturing fluid–solid interactions, that couples a Boundary Element (BE) approach for solid viscoelastic deformation and a finite difference scheme for fluid flow dynamics, with good agreement with experimental results (Stupkiewicz et al., 2016).

It is evident that these interactions occurring at the lubricated interfaces are critical in a variety of contexts, including power transmission components: indeed, the role of lubrication is fundamental

\* Corresponding author at: Department of Mechanics, Mathematics and Management, Politecnico di Bari, Via Orabona 4, 70100, Bari, Italy.  
E-mail address: [carmine.putignano@poliba.it](mailto:carmine.putignano@poliba.it) (C. Putignano).

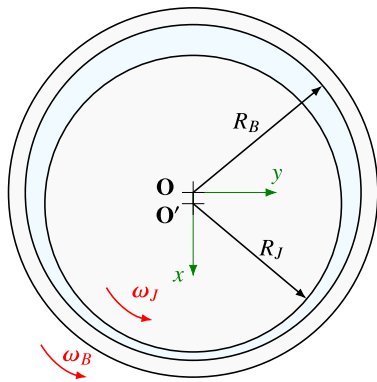


Fig. 1. Schematic of the journal bearing.

in rotor dynamics applications, as it reduces the level of wear of the contacting pairs. Journal bearings are, indeed, crucial components in a variety of industrial applications. Indeed, they are commonly used in various subsystems in engines and power trains, such as for crankshaft and camshaft: the piston pin-bore bearing and the big-end bearings are just possible examples (Crolla, 2009; Rahnejat, 2010). These components are also critical in the aerospace industry, in the rocker shaft of rocker-arm valve train systems, or in industrial turbines for power generation (Chasalevris and Dohnal, 2016). Hence, researchers worldwide made significant efforts to reach a comprehensive understanding of the journal bearings performances under different operating conditions (Reynolds, 1886; Hamrock et al., 2004; Linjamaa et al., 2018; Eder et al., 2018; Boidi et al., 2020; Ielchici et al., 2020). The theoretical analyses of the elastic distortion of journal bearings were motivated by the experimental work of Carl (1964), who was able to investigate the impact of elastic deformations, i.e., the cavitation angle rises, the pressure peak falls, and the minimum film thickness point shifts toward the maximum pressure location. Higginson (1965) investigated the performances of a journal bearing with a thin elastic layer, but the simplified treatment of the elastic problem, assuming the distortions to be proportional to the locally applied pressure, led to notable discrepancies with the actual bearing performances. The latter were addressed by Donoghue et al. O'Donoghue et al. (1967), where the authors provided an effective approach to the elastohydrodynamic problem for an infinitely long journal bearing in the presence of an isoviscous fluid, achieving extremely good agreement with experimental results (Carl, 1964). The problem of the compliant journal bearing was also investigated by Benjamin and Castelli (1971), who faced the elastic problem with different methods, while Hooke and O'donoghue (1972) assessed the EHL problem of soft materials, observing, for an elastomer lined journal bearing, deviations of the pressure distribution from the Hertzian solution as the eccentricity ratio is increased: the film thickness becomes negligible with respect to the deformation of the soft surface. Furthermore, relevant studies were carried out by Oh and Huebner (1973), who further explored the lubrication of a finite-length flexible bearing using a finite-element technique, and by Conway et al. in Conway and Lee (1975), Mak and Conway (1977), Conway and Lee (1977). In particular, in Conway and Lee (1975), the authors investigated the elasticity effect in an infinitely long bearing, assuming, at first, that the lubricant is isoviscous and, then, extending the investigation to the case of a pressure-dependent viscosity. In addition, as made by Higginson (1965), the authors made the hypothesis that the radial deformation linearly depends on the pressure distribution. On the other hand, in Mak and Conway (1977), the lubrication of a long, porous, deformable journal bearing was also investigated: the response of the bearing, provided the bearing shell thickness to be much smaller than the peripheral length of the bearing, has been modeled as a Winkler foundation. In Conway and Lee (1977), the

same approach has been used to assess the performance of a short flexible journal bearing. Furthermore, Profito (Profito and Zachariadis, 2015; Profito et al., 2019) proposed a Finite Volume Method based on Elements (FVMbE) scheme to assess statically loaded journal bearing, with particular attention to the case of a typical internal combustion engine connecting rod big-end bearing.

Crucially, this huge variety of theoretical and numerical efforts to fully understand the response of journal bearings has focused on linear elasticity: however, due to the encroaching role of polymers in the present and coming industrial panorama, special attention to soft lubrication involving polymer-based materials is needed. To this regard, several experimental campaigns have been carried out and particular attention has been paid to water-lubricated rubber journal bearings, which can avoid oil spill due to leakage into critical environment. Indeed, with respect to oil-lubricated metal bearings, they can reduce the consumption of lubricating oil and, nonetheless, friction, wear, and noise. Moreover, these bearings can accommodate misalignments and are easy to maintain, due to their simple structure. These advantages explain why water-lubricated bearings are now commonly used in several rotating machineries, such as in military crafts propulsion systems (Orndorff, Jr., 1985; Cabrera et al., 2005; Liu and Li, 2021).

The level of theoretical understanding for polymer journal bearings and for the related frictional performances is, however, still insufficient: in particular, a clear assessment of the role played by the viscoelastic rheology associated with the soft bodies is still missing. Indeed, recent theoretical investigations (Putignano and Dini, 2017; Putignano, 2020) have shown the existence of a peculiar viscoelastic-hydrodynamic lubrication (VEHL) regime, where solid viscoelasticity determines a marked difference, in terms of pressure, film thickness and ultimately friction, compared to classic EHL. This has to be properly evaluated also for journal bearings. Thus, in this paper, we present a contribution in this direction by focusing our attention on the infinitely long polymer journal bearing sketched in Fig. 1. In particular, our goal is to understand the role of viscoelastic rheology in the steady-state operations of the bearing. The present methodology paves over the mathematical formulation introduced by the authors in Santeramo et al. (2023b) for conforming and non-conforming surfaces, based on the definition of the Green's function for the dry contact between a rigid pin rolling about the center of an infinite viscoelastic holed space. Specifically, the Green's function takes into account the circular characteristic of the contact domain. Hence, here we develop a Boundary Element Method (BEM) to numerically assess the lubricated contact in a journal bearing. Importantly, as it will be shown later, the definition of such Green's function is crucial: in fact, the employment of the classical half-plane Green's function (Hamrock et al., 2004; Carbone and Mangialardi, 2004; Carbone and Putignano, 2013) would lead to misleading solutions in terms of film thickness and pressure distribution, thus in terms of the bearing capacity and behavior of the system. Furthermore, it should be noted that the development of such BE techniques results in significantly lower computing complexity when compared to Finite Element approaches. This exacerbates when multiple scales are considered in the analysis.

The paper is organized as follows. Section 2 contains the mathematical formulation of the contact problem, and Section 3 presents the results for the polymer journal bearing, enlightening the importance of viscoelasticity on the bearing performances. Three different configurations are investigated. In the hard-on-soft configuration (HS) the shaft is assumed to be rigid and the bearing is soft. In the soft-on-hard configuration (SH), the shaft is soft and the bearing is rigid, and, finally, in the soft-on-soft configuration (SS) both the interacting pair are soft. Hence, we focus on the pressure and film thickness distributions, in the case of a hard-on-soft configuration, when the journal rotating speed is increased while keeping the angular speed of the bearing constant, showing how the coupling between solid viscoelasticity and fluid viscous losses significantly affects the bearing response.

## 2. Mathematical formulation

Lubricated contacts involving deformable bodies are characterized by a strong coupling between the elastic, or viscoelastic, problem governing the deformation of the bodies and the Reynolds equations. Specifically, the deformation experienced by the bodies is governed by the pressure distribution, which is the solution of the Reynolds equations. The latter is determined by the lubricating film thickness, which intrinsically takes into account the displacement field of the interacting pair. Now, before dealing with the equations governing pressure and film thickness distributions, it is useful to recall how linear viscoelastic materials can be modeled from a mechanical point of view (Christensen, 2012). In particular, under isothermal conditions, the constitutive relation between stress and strain is:

$$\varepsilon(t) = \int_{-\infty}^t d\tau J(t-\tau)\dot{\sigma}(\tau) \quad (1)$$

where  $\varepsilon(t)$  denotes the time-dependent strain, and  $\dot{\sigma}(t)$  is the time derivative of the stress. Moreover,  $J(t)$  is the so-called creep function, which satisfies the causality principle, namely  $J(t < 0) = 0$ . As shown by Christensen (Christensen, 2012),  $J(t)$  is equal to:

$$J(t) = \mathcal{H}(t) \left[ 1/E_0 - \int_0^{+\infty} d\tau C(\tau) \exp(-t/\tau) \right] \quad (2)$$

where  $E_0$  is the rubbery modulus of the viscoelastic material,  $C(t)$  is the creep spectrum,  $\tau$  is the relaxation time, and  $\mathcal{H}(t)$  is the Heaviside step function. To characterize any real viscoelastic material, in numerical simulations, Eq. (2) is generally discretized:

$$\begin{aligned} J(t) &= \mathcal{H}(t) \left[ 1/E_0 - \sum_{k=1}^n C_k \exp(-t/\tau_k) \right] \\ &= \mathcal{H}(t) \left[ 1/E_\infty + \sum_{k=1}^n C_k (1 - \exp(-t/\tau_k)) \right] \end{aligned} \quad (3)$$

with  $E_\infty$  being the high-frequency modulus, or glassy modulus, of the material.

Thus, let us focus on the contact problem under analysis and determine the bearing response under steady-state operating conditions. In particular, we move from the mathematical formulation presented in Santeramo et al. (2023b), where the authors proposed a Green's function approach to assess steady-state viscoelastic circular contacts.

Now, under the assumptions that the solids are homogeneous and the viscoelastic properties do not show any spatial dependency, recalling that the system is invariant under rotations and the elastic-viscoelastic correspondence principle (Lakes, 2009; Christensen, 2012; Carbone and Putignano, 2013; Putignano, 2021), we can express, in a polar coordinate system, the relationship between the total displacement  $\mathbf{u} = u_r \mathbf{e}_r + u_\theta \mathbf{e}_\theta$  and the stress  $\boldsymbol{\sigma} = \sigma_r \mathbf{e}_r + \sigma_\theta \mathbf{e}_\theta$ :

$$\mathbf{u}(s, t) = \int_{-\infty}^t dt' \int_0^{2\pi R} ds' J(t-t') \mathbf{G}(s-s') \dot{\boldsymbol{\sigma}}(s', t'), \quad (4)$$

with  $R$  being the radius of the particular contact domain,  $s = R\theta$  and  $s' = R\theta'$ . Moreover,  $t$  is the time and  $\mathbf{G}(s)$  is the spatial Green's tensor. From Eq. (4), it can be noticed that inertial effects have been neglected.

Thus, recalling that the hysteretic losses are governed by the normal contact pressure, we focus on the normal contact problem. Specifically, as presented in detail in Santeramo et al. (2023b), we can then rephrase Eq. (4) as:

$$u_r(S) = \int_0^{2\pi R} ds' \mathcal{G}_{rr}(S-S', \omega) \sigma_r(S'), \quad (5)$$

with  $\omega$  being the velocity of the contact patch,  $S = s - \omega Rt$  and  $S' = s' - \omega Rt$ . Furthermore,  $\mathcal{G}_{rr}(S)$  is the so-called viscoelastic steady-state Green's function, which is equal to:

$$\begin{aligned} \mathcal{G}_{rr}(S) &= J(0)G_{rr}(S) \\ &+ \int_0^{+\infty} d\tau C(\tau) \int_0^{2\pi/\omega\tau} d\zeta e^{-\zeta} G_{rr}(S + \omega R\tau\zeta). \end{aligned} \quad (6)$$

Then, making use of Eq. (5), we can specify the displacement field for the bearing profile as:

$$u_r^B(S) = \int_0^{2\pi R_B} ds' \mathcal{G}_{rr}^B(S-S', \bar{\omega}_B) \sigma_r(S'), \quad (7)$$

where  $\bar{\omega}_B$  denotes the velocity of the contact patch at the bearing interface.

$\mathcal{G}_{rr}^B$  is determined by substituting  $G_{rr}(S)$  in Eq. (6) with the following expression:

$$\begin{aligned} \mathcal{G}_{rr}^B(s) &= \frac{1+\nu}{2\pi} \left[ -\frac{\kappa}{\kappa+1} (2 \log R_B + 1) \cos \theta \right. \\ &\quad \left. - \frac{\kappa+1}{2} B(\theta) \cos \theta + (\kappa-1) A(\theta) \sin \theta \right], \end{aligned} \quad (8)$$

with  $\nu$  being the Poisson's ratio,  $\kappa$  is the Kolosov's constant, which is equal to  $\kappa = 3 - 4\nu$ , as the problem under investigation is a plane strain problem. Furthermore,  $A(\theta) = \arg(1/2 - i/2 \cot(\theta/2))$  and  $B(\theta) = \log(2 - 2 \cos \theta) = 2 \log(2 |\sin(\theta/2)|)$ , with  $\theta = s/R_B$  being the angle subtended by the arc  $s$ . More details about the derivation of the spatial Green's function in Eq. (8) can be found in Santeramo et al. (2023b).

On the other hand, the journal displacement field is described by:

$$u_r^J(S) = \int_0^{2\pi R_J} ds' \mathcal{G}_{rr}^J(S-S', \bar{\omega}_J) \sigma_r(S'), \quad (9)$$

in which  $\bar{\omega}_J$  is the velocity of the contact patch at the journal interface.

Now,  $\mathcal{G}_{rr}^J$  is determined by setting  $G_{rr}(S)$  in Eq. (6) as:

$$\begin{aligned} \mathcal{G}_{rr}^J(s) &= \frac{1+\nu}{2\pi} \left[ \frac{1 - (\kappa^2 + 1) \log R_J}{\kappa + 1} \cos \phi - \cos \phi - \frac{\kappa + 1}{2} \right. \\ &\quad \left. + (\kappa - 1) A'(\phi) \sin \phi - \frac{\kappa + 1}{2} B(\phi) \cos \phi \right], \end{aligned} \quad (10)$$

with  $A'(\phi) = \arg(-1/2 - i/2 \cot(\phi/2))$ , and  $\phi = s/R_J$ . The detailed derivation of  $\mathcal{G}_{rr}^J(s)$  can be found in Santeramo et al. (2023a).

Hence, to numerically solve the contact problem, we employ the numerical scheme proposed in Carbone and Putignano (2013), Santeramo et al. (2023a,b): the contact domain is discretized with  $N$  elements, and assuming that the discretization step is small enough to consider the stress  $\sigma_k$  constant and equal to  $\sigma_k = \sigma_r(S_k)$  on the arc  $[S_k - \alpha R, S_k + \alpha R]$ , we can write the displacement of the  $i$ th interval as  $\{u_i\} = [L_{ik}(\omega)] \{\sigma_k\}$ . Therefore, it is possible to rephrase Eqs. (7) and (9) as the following linear systems (Santeramo et al., 2023a):

$$\{u_i^B\} = [L_{ik}^B(\bar{\omega}_B)] \{\sigma_k\} \quad (11a)$$

$$\{u_i^J\} = [L_{ik}^J(\bar{\omega}_J)] \{\sigma_k\} \quad (11b)$$

Furthermore, the intercorrelation matrix entries  $L_{ik}^B$  and  $L_{ik}^J$  are defined as  $L_{ik}^B = L_{rr}^B(S_i - S_k, \bar{\omega}_B)$  and  $L_{ik}^J = L_{rr}^J(S_i - S_k, \bar{\omega}_J)$ , which are equal to:

$$\begin{aligned} L_{rr}^B(S) &= J(0)L_{rr}^B(S) \\ &+ \int_0^{+\infty} d\tau C(\tau) \int_0^{2\pi/\bar{\omega}_B\tau} dz e^{-z} L_{rr}^B(S + \bar{\omega}_B R_B \tau z), \end{aligned} \quad (12a)$$

$$\begin{aligned} L_{rr}^J(S) &= J(0)L_{rr}^J(S) \\ &+ \int_0^{+\infty} d\tau C(\tau) \int_0^{2\pi/\bar{\omega}_J\tau} dz e^{-z} L_{rr}^J(S + \bar{\omega}_J R_J \tau z), \end{aligned} \quad (12b)$$

in which

$$L_{rr}^B(S) = \int_0^{2\pi R_B} ds' G_{rr}^B(S-S') \chi_r(S'), \quad (13a)$$

$$L_{rr}^J(S) = \int_0^{2\pi R_J} ds' G_{rr}^J(S-S') \chi_r(S'), \quad (13b)$$

where, with reference to the particular contact problem,  $\chi_r$  denotes a unitary pressure distribution in the arc  $[-\alpha R, \alpha R]$  (Santeramo et al., 2023b).

Once the system of linear equations governing the solid viscoelastic problem is set, we can focus on the equations that govern the fluid dynamics of the system. To this regard, considering isoviscous fluids,

and assuming no-slip boundary conditions at both solids interfaces, the Reynolds equations in a polar reference frame can be written as (Venner and Lubrecht, 2000; Hamrock et al., 2004):

$$\frac{\partial}{\partial s} \left( h^3 \frac{\partial \sigma}{\partial s} \right) = 12 \bar{v} \eta \frac{\partial h}{\partial s}, \quad (14)$$

where  $\bar{v}$  is the entrainment speed, computed as the average of the peripheral velocities of the surfaces, namely  $\bar{v} = (\mathbf{v}_B + \mathbf{v}_J)/2$ , in which  $\mathbf{v}_B$  and  $\mathbf{v}_J$  denote the peripheral velocity of a generic point on the bearing and on the shaft respectively, namely  $\mathbf{v}_B(\theta) = \boldsymbol{\omega}_B \wedge (\mathbf{P}_B(\theta) - \mathbf{O})$  and  $\mathbf{v}_J(\theta) = \boldsymbol{\omega}_J \wedge (\mathbf{P}_J(\theta) - \mathbf{O}')$ . Moreover,  $h$  is the film thickness, and  $\eta$  is the fluid viscosity. Specifically, the normal displacement of the interacting pair profiles strongly affects the film thickness distribution. Indeed, we have that  $h(\theta) = h_0 + g_0(\theta) + u_r^B(\theta) - u_r^J(\theta)$ , with  $h_0$  and  $g_0(\theta)$  being respectively the central film thickness and the gap between the surfaces of the bodies in the undeformed configuration. For the system under analysis in this paper, that is the journal bearing,  $g_0(\theta) = c(1 - \epsilon \cos(\theta))$  (Hamrock et al., 2004; Harris, 2007), where  $c$  is the bearing radial clearance, i.e.  $c = R_B - R_J$ , and  $\epsilon$  is the eccentricity ratio, that is equal to  $\epsilon = e/c$ , with  $e$  being the eccentricity, which is equal to  $e = |\mathbf{O}' - \mathbf{O}|$ . As shown in Hamrock et al. (2004) the previous definition of  $g_0(\theta)$  holds for highly conforming profiles, i.e. for very small  $e/R_B$  ratios. When this condition is not met, a proper definition of the separation  $g_0$  is needed (Hamrock et al., 2004). In addition, to take into account hydrodynamic cavitation in the divergent section, where the lubricant is subject to a tensile stress situation, Reynolds boundary conditions (Hamrock et al., 2004) are employed. Then, Eq. (14) is attacked by implementing a finite difference scheme (Venner and Lubrecht, 2000; Hamrock et al., 2004), thus obtaining the following vector equation:

$$h_i = R_{ik}(\bar{v}, \eta) \sigma_k. \quad (15)$$

Thus, to assess the contact problem, we need to couple the solid mechanics and the fluid dynamics (Elsharkawy, 1996; Venner and Lubrecht, 2000; Hamrock et al., 2004; Putignano et al., 2019) to determine the pressure distribution satisfying, at the same time, both Eq. (11) and Eq. (15). In particular, an iterative scheme underrelaxed with the Aitken acceleration approach (Irons and Tuck, 1969; Venner and Lubrecht, 2000; Profito and Zachariadis, 2015; Profito et al., 2019) is implemented: starting from the film thickness estimation  $\tilde{h}_n$ , computed at the previous step, an estimated stress field  $\tilde{\sigma}_k$  is obtained by inverting Eq. (15), and the new displacement field can be determined from Eq. (11). Finally, it is possible to compute the film thickness  $\tilde{h}_{n+1}$  for the subsequent iteration, and the iterative process continues until the pressure distribution numerically converges in two consecutive iterations.

Ultimately, it is possible to focus our analysis to the friction losses, which can be determined as the combination of the viscoelastic hysteretic dissipation and the fluid losses (Hamrock et al., 2004). Specifically, for each body, we can determine the net force and the total torque respectively as:

$$\mathbf{F}_{tot} = \mathbf{F}_n + \mathbf{F}_\tau = R \left[ \int_0^{2\pi} d\theta p(\theta) \mathbf{n}(\theta) + \int_0^{2\pi} d\theta \tau(\theta) \mathbf{t}(\theta) \right], \quad (16)$$

and

$$\mathbf{C}_\tau = R \int_0^{2\pi} d\theta (\mathbf{P}(\theta) - \mathbf{O}) \wedge (p(\theta) \mathbf{n}(\theta) + \tau(\theta) \mathbf{t}(\theta)), \quad (17)$$

where  $\mathbf{O}$  denotes the bearing center, that corresponds to the origin of the frame of reference sketched in Fig. 1, and  $\mathbf{P}(\theta)$  is the point, at angular coordinate  $\theta$ , of the deformed contour. Moreover,  $\mathbf{n}(\theta)$  and  $\mathbf{t}(\theta)$  are the unit vectors, respectively normal and tangential to the deformed profile; ultimately,  $p = \sigma$ , and the viscous shear stresses  $\tau$  acting on the bearing surface, i.e.  $\tau = \tau_B$ , and on the journal surface, i.e.  $\tau = \tau_J$ , are obtained as (Hamrock et al., 2004):

$$\tau_B(\theta) = -\frac{h}{2R_B} \frac{\partial p}{\partial \theta} - \frac{\eta(\mathbf{v}_B(\theta) - \mathbf{v}_J(\theta))}{h}, \quad (18a)$$

$$\tau_J(\theta) = -\frac{h}{2R_J} \frac{\partial p}{\partial \theta} + \frac{\eta(\mathbf{v}_B(\theta) - \mathbf{v}_J(\theta))}{h}. \quad (18b)$$

Finally, it is of particular interest to quantify the viscoelastic contribution to friction. Specifically, it is possible to compute the power related to viscoelastic dissipation  $P_{v,d}$ , which is equal to:

$$P_{v,d} = \omega R \int_0^{2\pi} d\theta p(\theta) \frac{\partial u_r(\theta)}{\partial \theta}. \quad (19)$$

### 3. Numerical results

In this Section, in order to point out the implications of the approach previously developed, we consider a journal bearing operating in steady-state conditions, where the bearing has a radius equal to  $R_B = 0.1$  m, and the radial clearance  $c$  is equal to  $c = R_B - R_J = 5 \cdot 10^{-4}$  m. Specifically, when referring to soft solids in the following study, we employ a single relaxation time material with glassy modulus  $E_\infty = 100$  MPa,  $E_\infty/E_0 = 100$ , and relaxation time  $\tau = 1$  s.

As a first step, we investigate a classic Elastohydrodynamic lubrication (EHL) problem: the journal is rigid and the bearing is elastic with elastic modulus being equal to the rubbery modulus  $E_0$ , and Poisson's ratio  $\nu = 0.5$ , while the fluid is isoviscous with a viscosity  $\eta$  being equal to  $\eta = 0.001$  Pa · s. As pointed out in Fig. 2 for a dimensionless net force  $\tilde{F}_{tot} = |\mathbf{F}_{tot}|/E_0 R_B = 2.2 \cdot 10^{-3}$ , the solution in terms of dimensionless film thickness and pressure distributions (solid lines), defined respectively as  $\tilde{h} = h/c$  and  $\tilde{p} = p/E_0$ , differs from what we would obtain by solving the classical non-conformal EHL problem, that is, by employing the usual half-plane Green's function to compute the elastic deformation of the solids (Johnson and Johnson, 1987; Barber, 2002; Carbone and Mangialardi, 2004) (dashed lines). Crucially, we can conclude that the half-plane approximation is not suitable for lubricated conformal contact problems and justify the necessity of developing a numerical method properly tuned. This aspect is of the utmost importance when the bearing response is analyzed, and it must be carefully taken into account in design processes.

Now, we can focus on the analysis of the viscoelasticity effects for a polymer journal bearing. In particular, we investigate three different contact conditions: rigid journal on soft bearing liner (HS), soft journal on rigid bearing liner (SH), and soft journal on soft bearing liner (SS). As shown in Fig. 3, the pressure and film thickness distributions are dramatically affected by the choice of material pairing: it is thus clear that viscoelasticity plays a pivotal role. Crucially, this leads to a different attitude angle of the resulting force (red arrows in Fig. 3), i.e. the angle the net force generates with respect to the line of centers (Hamrock et al., 2004), and, ultimately, on the angular position of the application point. Clearly, such a variation in the resultant force has important consequences on the rotor dynamics of the entire system where the bearing is applied. Calculations are carried out for dimensionless speeds for the bodies being respectively equal to  $\tilde{\omega}_B = \omega_B \tau = 0.2$  and  $\tilde{\omega}_J = \omega_J \tau = -0.4$ , while keeping the dimensionless resultant force  $\tilde{F}_{tot}$  constant and equal to  $\tilde{F}_{tot} = 2.2 \cdot 10^{-3}$ : the Hersey parameter  $H$  is then equal to  $H = \eta \tilde{v} R_B / |\mathbf{F}_{tot}| = -4.5 \cdot 10^9$ . Thus, starting with the HS configuration, we observe a clear peak in the pressure distribution at the leading edge due to solid viscoelasticity. Incidentally, the leading edge of the solid contact corresponds to the flow outlet, i.e. where the lubricant exits the lubricated contact. Here, we find a minimum in the film thickness, due to both flow conservation and the viscous resistance against the instantaneous change of deformation.

When we consider the SH case, we retrieve a very different outcome. Now, the bearing is rigid, while the journal is linear viscoelastic and, coherently with the kinematics of the problem, we have that the fluid inlet, i.e. where the fluid is sucked in the contact, corresponds to the leading edge for the journal: hence, the peak in the pressure distribution. Finally, in the SS configuration, both the contacting pairs are linear viscoelastic and, since the system is now more compliant, the contact region is now larger than that observed in the previous

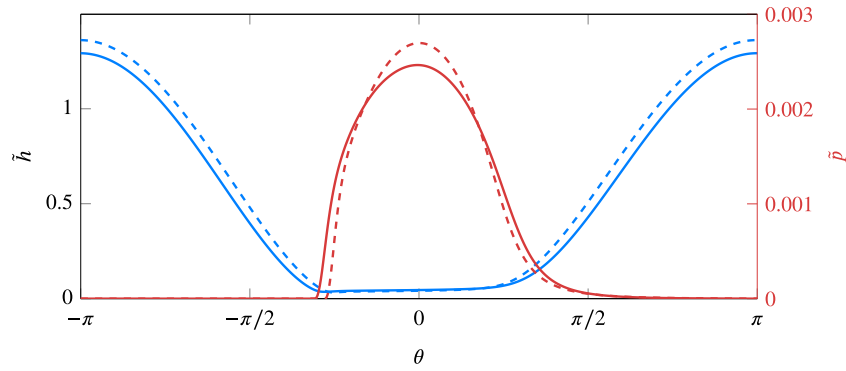


**Fig. 2.** The dimensionless film thickness  $\tilde{h} = h/c$  (blue) and pressure  $\tilde{p} = p/E_0$  (red) distributions for a fixed value of the dimensionless resultant force  $\tilde{F}_{tot} = |\mathbf{F}_{tot}|/E_0 R_B = 2.2 \cdot 10^{-3}$ . The numerical predictions are carried out in EHL regime, where the journal is rigid and the bearing is elastic, with elastic modulus  $E = 1$  MPa and Poisson's ratio  $\nu = 0.5$ , and compared with the solution obtained using the half-plane Green's function (dashed lines).

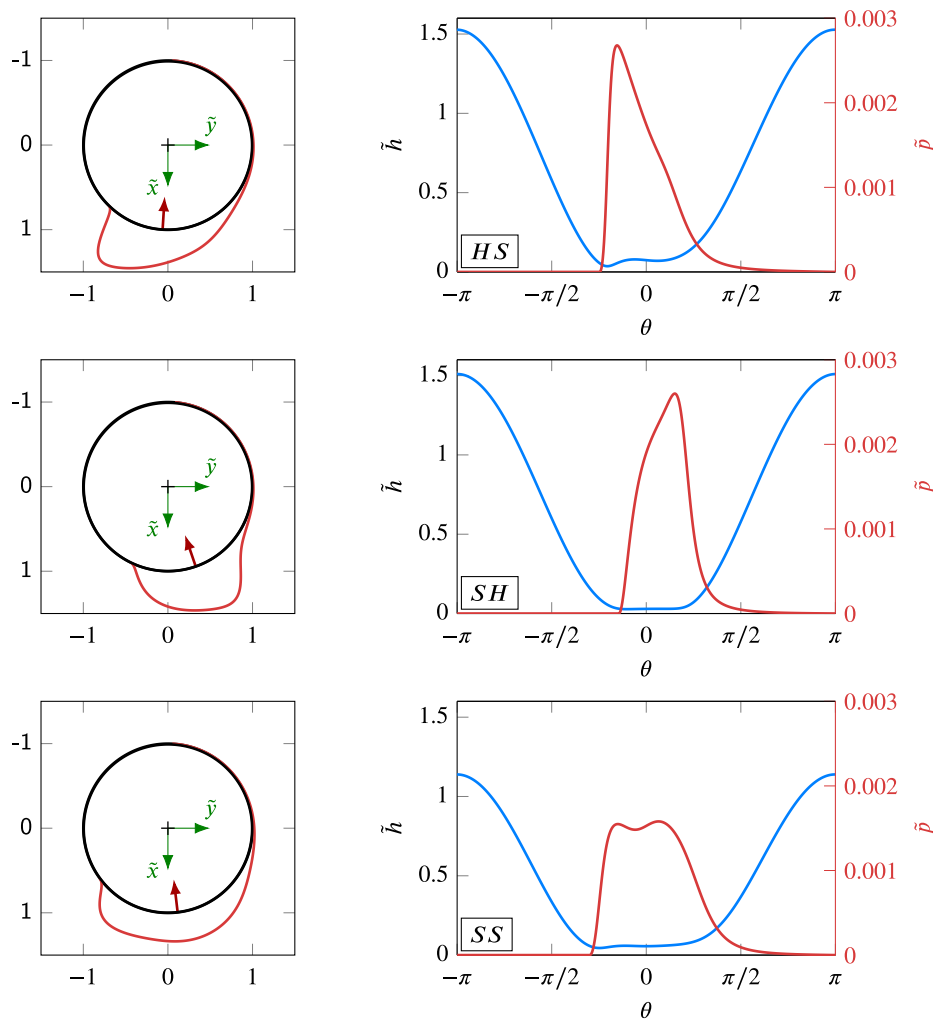


**Fig. 3.** The deformed profile (solid black line), the pressure distribution (solid red line) and the resulting net force  $F_{net}$  (red arrow) on the left; the dimensionless film thickness  $\tilde{h} = h/c$  (solid blue line) and the dimensionless pressure  $\tilde{p} = p/E_0$  (solid red line) distributions on the right. The results are carried out for a fixed value of the Hersey number  $H = -4.5 \cdot 10^9$  and three different configurations: hard-on-soft (HS), soft-on-hard (SH) and soft-on-soft (SS), with  $\tilde{\omega}_B = 0.2$  and  $\tilde{\omega}_J = -0.4$ . The axes  $\tilde{x}$  and  $\tilde{y}$  refer to the normalized  $x$ - and  $y$ -coordinates, i.e.,  $\tilde{x} = x/R_B$  and  $\tilde{y} = y/R_B$ .

cases. Furthermore, looking at the pressure distribution, it is possible to notice two peaks at the inlet and at the outlet of the contact zone, corresponding to the leading edges of the journal and the bearing

respectively. To this regard, the reader should observe that, for each viscoelastic body, the leading edge is the region where the contact is initiated and where a larger stiffness and, thus, a larger pressure are

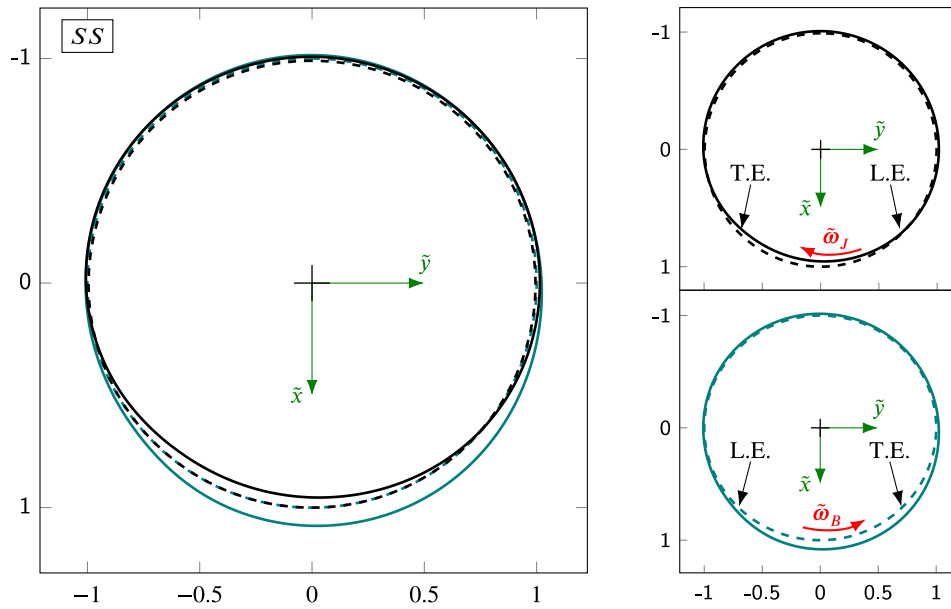


Fig. 4. The undeformed (dashed lines) and the magnified deformed (solid lines) contours of the journal (black) and the bearing (teal), with  $K = 50$  being the magnification factor. The calculations are carried out for a soft-on-soft (SS) configuration, with a fixed value of the Hersey number  $H = -4.5 \cdot 10^9$ , and  $\tilde{\omega}_B = 0.2$  and  $\tilde{\omega}_J = -0.4$ . The axes  $\tilde{x}$  and  $\tilde{y}$  refer to the normalized  $x$ - and  $y$ -coordinates, i.e.,  $\tilde{x} = x/R_B$  and  $\tilde{y} = y/R_B$ . The arrows refer to the leading (L.E.) and trailing (T.E.) edges for each viscoelastic solid.

shown (Carbone and Putignano, 2013). Indeed, as Fig. 4 shows for the latter case, which refers to a soft journal on a soft bearing, the location of the leading regions can be elicited from superposing the undeformed contours (dashed lines) and the deformed contours (solid lines) of the bodies: the region where the deformed profile, magnified to improve the readability of the figure, is closer to the undeformed contour corresponds to the leading edge (L.E.) zone, while larger displacements are observed at the trailing edge (T.E.), where the material is still relaxing upon the passage of the load. In fact, looking at the right panel of Fig. 4, it is straightforward to find the leading region for the shaft (in black) at the fluid inlet, i.e. on the right, where the minimum deviation between deformed and undeformed profile occurs; on the contrary, for the bearing (in green) this condition is met at the fluid outlet, while large deviations between the actual (deformed) and the reference (undeformed) profiles are retrieved at the fluid inlet, which corresponds to the trailing edge. Hence it is clear that, in viscoelastic lubricated contacts, besides the Hersey number  $H$ , the dimensionless speeds of the interacting pair, i.e.  $\tilde{\omega}_B$  and  $\tilde{\omega}_J$ , are fundamental in governing the response of the system, since they capture the complex rheology of such materials.

Now, it is interesting to study the system response when the absolute value of the shaft angular speed  $|\tilde{\omega}_J|$  increases, while keeping fixed the total load  $\tilde{F}_{tot} = 2.2 \cdot 10^{-3}$  and the bearing angular speed  $\tilde{\omega}_B = 0.2$ . Specifically, we focus on a hard-on-soft (HS) configuration, where the shaft is considered rigid, while the bearing liner is linear viscoelastic. Crucially, the impact of viscoelasticity effects on the bearing performance is quite evident, as shown in Fig. 5. A clear asymmetry in the pressure distribution occurs due to the different relaxation between leading and trailing edges; in particular, the leading edge for the bearing is located at the fluid outlet, where a peak in the pressure distribution and, correspondingly, a minimum in the film thickness distribution are retrieved. As soon as we increase the shaft angular velocity, the fluid load-bearing capacity increases since more lubricant is entrained in the lubricated contact zone. Hence, the reduced values of the maximum pressure and the very peculiar film thickness distributions, the latter characterized by increasing values of the central film thickness  $h_0$ , and by a certain degree of asymmetry related to the viscoelastic response of the bearing material. Ultimately, the upper graph in Fig. 6 presents, on the left  $y$ -axis, the resisting torque

parameter for the bearing, i.e.  $\chi_B = C_B/|\mathbf{F}_{tot}|R_B$ , and for the journal, i.e.  $\chi_J = C_J/|\mathbf{F}_{tot}|R_B$ , computed as presented in Section 2 with respect to bearing center  $\mathbf{O}$ . Incidentally, it is of particular interest to highlight the viscoelastic contribution to the resisting torque parameter for the bearing, i.e.  $\chi_{v,B} = C_{v,B}/|\mathbf{F}_{tot}|R_B$ , directly obtained by the computation of the power related to the viscoelastic dissipation (see Eq. (19)): it is evident how the viscoelastic contribution to the overall bearing torque is important, especially at low shaft speeds. Indeed, as discussed beforehand, if the entrainment speed increases, the load-bearing capacity of the lubricant is enhanced: the bearing liner experiences lower levels of deformation and, consequently, the bulk energy dissipation diminishes. Furthermore, on the right  $y$ -axis of the former graph, the eccentricity ratio  $\epsilon$  as a function of the angular speed of the shaft  $|\tilde{\omega}_J|$  is depicted. In particular, it can be noticed that it follows a monotonic trend and, coherently with an increasing lubricant entrainment in the lubricated contact zone, we have higher values of the central fluid film thickness and, thus, lower values of the eccentricity ratio.

With regards to the influence of the applied load, as clear in the upper panels, for a fixed value of dimensionless speed  $\tilde{\omega}_B$ , the resisting torque parameter decreases with the load consistently with what is observed in a classic Stribeck curve for the friction coefficient. On the other hand, the viscoelastic hysteresis has to grow with the load, given the larger deformation and the related dissipation: as a result, the relative fraction of  $\chi_B$  due to the viscoelastic frictional effects, that is  $\chi_{v,B}/\chi_B$ , increases with the load and may go up to 65% for an applied load equal to  $\tilde{F}_{tot} = 4 \cdot 10^{-3}$ .

#### 4. Conclusions

In this paper, we have developed a Boundary Element approach to assess the lubricated contact problem of a polymer journal bearing operating in steady-state conditions. Crucially, the aim of this study is to highlight how viscoelasticity strongly affects the quantities that characterize the bearing performances, such as pressure, film thickness, and friction. To this end, a proper definition of the Green's functions is needed: this is clear when we focus on a journal bearing in elasto-hydrodynamic lubrication (EHL) regime, where the shaft is considered rigid, while the bearing liner is elastic. The numerical outcomes are compared, in terms of fluid film thickness and pressure distributions,

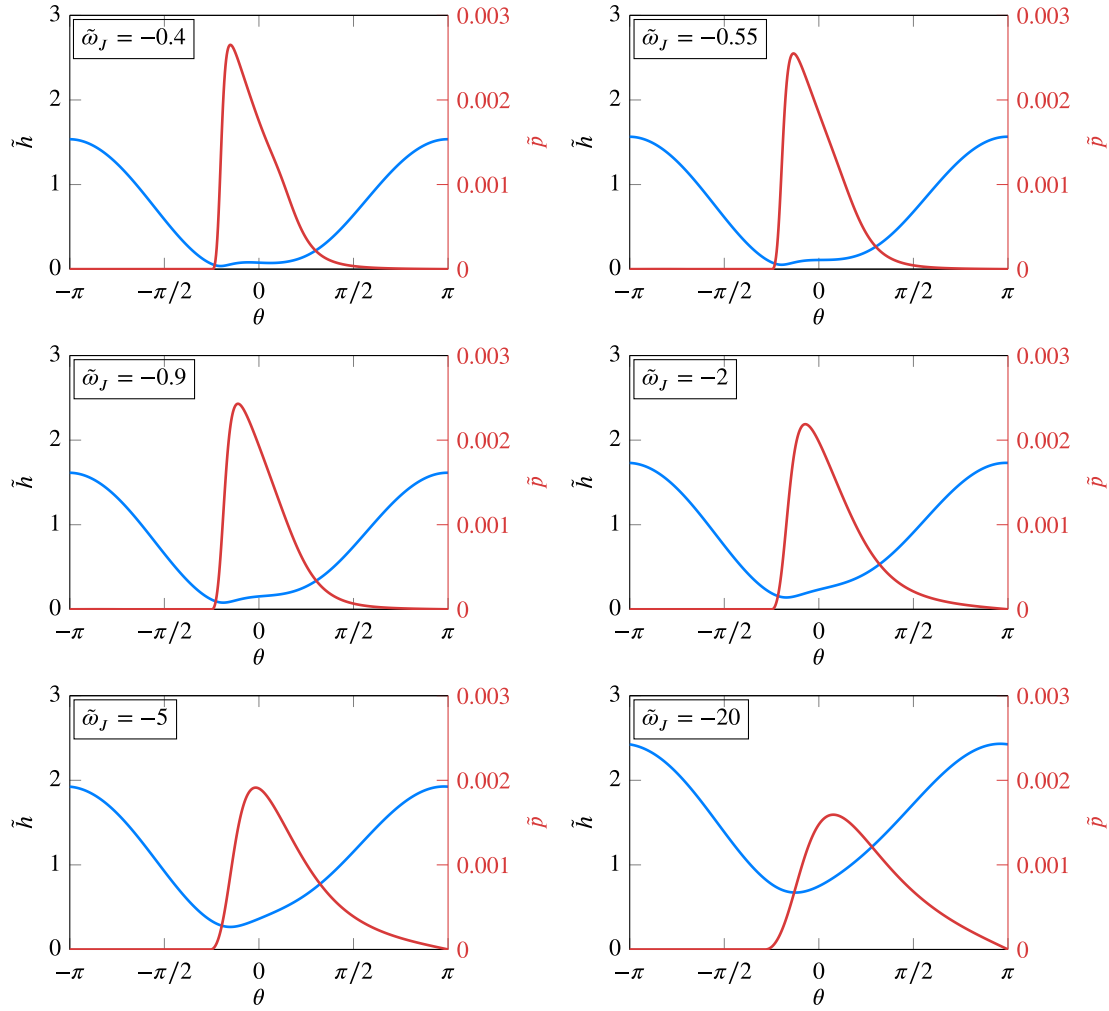


**Fig. 5.** The dimensionless film thickness  $\tilde{h} = h/c$  (solid blue line) and the dimensionless pressure  $\tilde{p} = p/E_0$  (solid red line) distributions at different journal speed  $\tilde{\omega}_J$  for a fixed value of the net force  $F_{tot}$ . The calculations are carried out for a hard-on-soft (HS) configuration, and a fixed  $\tilde{\omega}_B = 0.2$ .

with what is obtained by employing the half-plane Green's function: considerable deviations are observed, showing that the latter is not appropriate to analyze such a conforming circular contact problem. Further, we focus on the VEHL case and we show that the contact configuration is critical in determining the system response. Three different configurations have been considered, respectively the hard-on-soft configuration (HS), in which the shaft is rigid and the bearing is linear viscoelastic, soft-on-hard configuration (SH), in which the shaft is linear viscoelastic and the bearing is rigid, and the soft-on-soft configuration (SS), where both the solids are linear viscoelastic: dramatic changes are retrieved in the pressure and fluid film thickness distributions, thus on friction. In particular, the HS case has been further investigated, for a fixed value of the net force  $F_{tot}$  and a constant angular speed of the bearing  $\tilde{\omega}_B$ , while increasing the angular speed of the shaft  $|\tilde{\omega}_J|$ , showing the significant impact of the complex rheology of the viscoelastic bearing on the system behavior and, crucially, on friction. The latter is the result of the combination between fluid viscous losses and the viscoelastic hysteretic term. Thus, the resisting torque parameters for the bearing and the shaft are presented: for increasing values of the shaft angular velocity, higher values of the friction torque are obtained; conversely, we notice that the higher the shaft speed, the lower the eccentricity ratio. This is due to higher values of the central film thickness, as more fluid is entrained in the lubricated contact region.

Interestingly, we also quantify the power dissipation related to the hysteretic behavior of the viscoelastic material. This, in turn, enables us to quantify the contribution of the viscoelastic torque to the overall friction torque of the bearing. In particular, it has been observed that this contribution diminishes as the speed of the journal is increased, i.e., for larger values of the entrainment speed. This result is due to the lower deformation experienced by the material as the capacity of the lubricant to sustain the load increases. Furthermore, for increasing values of the applied load, the overall friction torque parameter  $\chi$  tends to decrease consistently with what is observed in the classic Stribeck curve, while the relative fraction due to the viscoelastic hysteresis grows given the larger bulk deformation and the consequent dissipation.

Ultimately, the results presented in this study underline that, in order to completely assess visco-elastohydrodynamic lubrication problems, the Hersey number is not the only parameter governing the system response, but the dimensionless speeds of the viscoelastic bodies, i.e.  $\tilde{\omega}_B$  and  $\tilde{\omega}_J$ , have to be taken into account carefully, as they embody the complex rheology of the materials. Indeed, as highlighted in this work, the bearing response changes dramatically as different contact configurations are considered, thus significantly affecting the rotor dynamics of the system in which the bearing is applied. As possible future developments, we observe that the present formulation can be further extended to include transient and thermal effects, as temperature plays a crucial role in the mechanical response of viscoelastic materials.

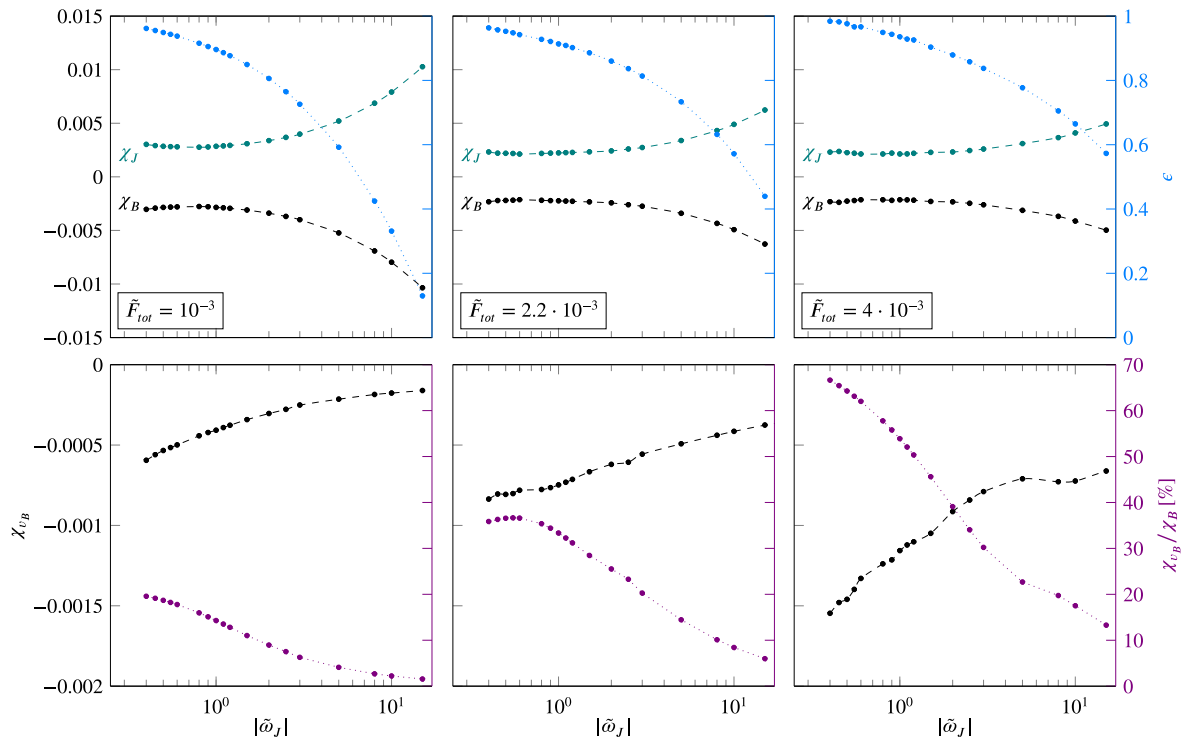


Fig. 6. In the upper panel, the resisting torque parameter for the journal  $\chi_J = C_J/|F_{tot}|R_B$  (green curve), for the bearing  $\chi_B = C_B/|F_{tot}|R_B$  (in black) on the left y-axis; on the right y-axis, the eccentricity ratio  $\epsilon$ . Below, the viscoelastic contribution to total resisting torque parameter for the bearing  $\chi_{v,b} = C_{v,b}/|F_{tot}|R_B$  (in black) on the left y-axis; the ratio  $\chi_{v,b}/\chi_B$  [%] on the right y-axis. The results are carried out for a hard-on-soft (HS) configuration at different journal dimensionless speed  $\bar{\omega}_J$ , and different levels of load  $\bar{F}_{tot}$ , respectively equal to  $\bar{F}_{tot} = 10^{-3}$  (left),  $\bar{F}_{tot} = 2.2 \cdot 10^{-3}$  (center), and  $\bar{F}_{tot} = 4 \cdot 10^{-3}$  (right). The bearing dimensionless speed is kept constant and equal to  $\bar{\omega}_B = 0.2$ .

### CRediT authorship contribution statement

**Michele Santeramo:** Writing – review & editing, Writing – original draft, Visualization, Validation, Software, Methodology, Investigation, Formal analysis, Data curation, Conceptualization. **Giuseppe Carbone:** Writing – review & editing, Validation, Supervision, Resources, Project administration, Methodology, Investigation, Funding acquisition, Formal analysis, Data curation, Conceptualization. **Georg Vorlauffer:** Writing – review & editing, Validation, Supervision, Resources, Project administration, Methodology, Investigation, Funding acquisition, Formal analysis, Conceptualization. **Stefan Krenn:** Writing – review & editing, Visualization, Validation, Supervision, Resources, Project administration, Methodology, Investigation, Funding acquisition, Formal analysis, Conceptualization. **Carmine Putignano:** Writing – review & editing, Visualization, Validation, Supervision, Software, Resources, Project administration, Methodology, Investigation, Funding acquisition, Formal analysis, Data curation, Conceptualization.

### Declaration of competing interest

The authors declare that they have no known competing financial interests or personal relationships that could have appeared to influence the work reported in this paper.

### Acknowledgments

This work was carried out as part of the COMET Centre InTribology project (FFG no. 872176 and 906860). InTribology is funded within the COMET — Competence Centres for Excellent Technologies Programme by the federal ministries BMK and BMAW as well as the federal states of Niederösterreich and Vorarlberg based on financial support from the project partners involved. COMET is managed by FFG. This work was also partly supported by the Italian Ministry of University and Research under the project “Super Polymer Bearings - SuperPolB” (Grant

No. CUP - D53D23003400006), and the Programme “Department of Excellence” Legge 232/2016 (Grant No. CUP - D93C23000100001). G. C. thanks the Italian Ministry of Education, University and Research and the European Union—NextGenerationEU (National Sustainable Mobility Center N00000023, Italian Ministry of University and Research Decree n. 1033—17/06/2022, Spoke 11—Innovative Materials & Lightweighting).

### Data availability

Data will be made available on request.

### References

- Askari, E., Andersen, M.S., 2018. A closed-form formulation for the conformal articulation of metal-on-polyethylene hip prostheses: Contact mechanics and sliding distance. *Proc. Inst. Mech. Eng. Part H: J. Eng. Med.* 232 (12), 1196–1208. <http://dx.doi.org/10.1177/0954411918810044>, PMID: 30445886.
- Barber, J., 2002. *Elasticity*. In: Online access with purchase: Springer, Springer Netherlands.
- Benjamin, M.K., Castelli, V., 1971. A theoretical investigation of compliant surface journal bearings.
- Boidi, G., Krenn, S., Eder, S.J., 2020. Identification of a material–lubricant pairing and operating conditions that lead to the failure of porous journal bearing systems. *Tribol. Lett.* 68, 1–14.
- Cabrera, D., Woolley, N., Allanson, D., Tridimas, Y., 2005. Film pressure distribution in water-lubricated rubber journal bearings. *Proc. Inst. Mech. Eng. Part J: J. Eng. Tribol.* 219 (2), 125–132.
- Carbone, G., Lorenz, B., Persson, B.N.J., Wohlers, A., 2009. Contact mechanics and rubber friction for randomly rough surfaces with anisotropic statistical properties. *Eur. Phys. J. E* 29 (3), 275–284. <http://dx.doi.org/10.1140/epje/i2009-10484-8>.
- Carbone, G., Mangialardi, L., 2004. Adhesion and friction of an elastic half-space in contact with a slightly wavy rigid surface. *J. Mech. Phys. Solids* 52 (6), 1267–1287. <http://dx.doi.org/10.1016/j.jmps.2003.12.001>.
- Carbone, G., Putignano, C., 2013. A novel methodology to predict sliding and rolling friction of viscoelastic materials: Theory and experiments. *J. Mech. Phys. Solids* 61 (8), 1822–1834. <http://dx.doi.org/10.1016/j.jmps.2013.03.005>.

- Carl, T.E., 1964. An experimental investigation of a cylindrical journal bearing under constant and sinusoidal loading. *Proc. Inst. Mech. Engrs* 178 (3), 100–119.
- Chasalevris, A., Dohnal, F., 2016. Improving stability and operation of turbine rotors using adjustable journal bearings. *Tribol. Int.* 104, 369–382.
- Christensen, R., 2012. *Theory of Viscoelasticity: An Introduction*. Elsevier.
- Conway, H., Lee, H., 1975. The analysis of the lubrication of a flexible journal bearing. Conway, H., Lee, H., 1977. The lubrication of short, flexible journal bearings.
- Crolla, D.A., 2009. *Automotive Engineering*.
- Dapp, W.B., Lücke, A., Persson, B.N.J., Müser, M.H., 2012. Self-affine elastic contacts: Percolation and leakage. *Phys. Rev. Lett.* 108, 244301. <http://dx.doi.org/10.1103/PhysRevLett.108.244301>.
- Eder, S., Ielchici, C., Krenn, S., Brandtner, D., 2018. An experimental framework for determining wear in porous journal bearings operated in the mixed lubrication regime. *Tribol. Int.* 123, 1–9. <http://dx.doi.org/10.1016/j.triboint.2018.02.026>.
- Elsharkawy, A.A., 1996. Visco-elastohydrodynamic lubrication of line contacts. *Wear* 199 (1), 45–53. [http://dx.doi.org/10.1016/0043-1648\(96\)07212-2](http://dx.doi.org/10.1016/0043-1648(96)07212-2).
- Friedrich, K., 2018. Polymer composites for tribological applications. *Adv. Ind. Eng. Polym. Res.* 1 (1), 3–39. <http://dx.doi.org/10.1016/j.aiepr.2018.05.001>.
- Fusaro, R., 1990. Self-lubricating polymer composites and polymer transfer film lubrication for space applications. *Tribol. Int.* 23 (2), 105–122. [http://dx.doi.org/10.1016/0301-679X\(90\)90043-O](http://dx.doi.org/10.1016/0301-679X(90)90043-O), Special Issue: Space Tribology.
- Grosch, K.A., 1963. The relation between the friction and visco-elastic properties of rubber. *Proc. R. Soc. Lond. Ser. A. Math. Phys. Sci.* 274 (1356), 21–39. <http://dx.doi.org/10.1098/rspa.1963.0112>.
- Hamrock, B.J., Jacobson, B., Schmid, S.R., 2004. *Fundamentals of Fluid Film Lubrication*. Taylor & Francis Inc.
- Harris, T.A., 2007. *Rolling bearing analysis*.
- Heeje, L., Gorb, S.N., 2014. Biologically inspired mushroom-shaped adhesive microstructures. *Annu. Rev. Mater. Res.* 44, 173–203.
- Heß, M., Forsbach, F., 2021. An analytical model for almost conformal spherical contact problems: Application to total hip arthroplasty with UHMWPE liner. *Appl. Sci.* 11 (23), <http://dx.doi.org/10.3390/app11231170>.
- Higginson, G., 1965. Paper 1: The theoretical effects of elastic deformation of the bearing liner on journal bearing performance. In: *Proceedings of the Institution of Mechanical Engineers, Conference Proceedings*, vol. 180, (2), SAGE Publications Sage UK: London, England, pp. 31–38.
- Hooke, C., 1997. Elastohydrodynamic lubrication of soft solids. In: Dowson, D., Taylor, C., Childs, T., Dalmaz, G., Berthier, Y., Flamand, L., Georges, J.-M., Lubrecht, A. (Eds.), *Elastohydrodynamics - '96 Fundamentals and Applications in Lubrication and Traction*. In: *Tribology Series*, vol. 32, Elsevier, pp. 185–197. [http://dx.doi.org/10.1016/S0167-8922\(08\)70448-6](http://dx.doi.org/10.1016/S0167-8922(08)70448-6).
- Hooke, C., O'donoghue, J., 1972. Elastohydrodynamic lubrication of soft, highly deformed contacts. *J. Mech. Eng. Sci.* 14 (1), 34–48.
- Hunter, S.C., 1961. The Rolling Contact of a Rigid Cylinder With a Viscoelastic Half Space. *J. Appl. Mech.* 28 (4), 611–617. <http://dx.doi.org/10.1115/1.3641792>.
- Ielchici, C.D., Krenn, S., Eder, S.J., 2020. A tribometer and methodology for wear and friction testing of porous journal bearings at elevated temperatures. *Ind. Lubr. Tribol.* 72 (8), 1027–1031.
- Irons, B.M., Tuck, R.C., 1969. A version of the aiken accelerator for computer iteration. *Internat. J. Numer. Methods Engrg.* 1 (3), 275–277.
- Johnson, K.L., Johnson, K.L., 1987. *Contact Mechanics*. Cambridge University Press.
- Koike, H., Kida, K., Santos, E., Rozwadowska, J., Kashima, Y., Kanemasu, K., 2012. Self-lubrication of PEEK polymer bearings in rolling contact fatigue under radial loads. *Tribol. Int.* 49, 30–38. <http://dx.doi.org/10.1016/j.triboint.2011.12.005>.
- Lakes, R., 2009. *Viscoelastic Materials*. Cambridge University Press, <http://dx.doi.org/10.1017/CBO9780511626722>.
- Linjamaa, A., Lehtovaara, A., Larsson, R., Kallio, M., Söchtig, S., 2018. Modelling and analysis of elastic and thermal deformations of a hybrid journal bearing. *Tribol. Int.* 118, 451–457.
- Liu, G., Li, M., 2021. Experimental study on the lubrication characteristics of water-lubricated rubber bearings at high rotating speeds. *Tribol. Int.* 157, 106868.
- Mak, W., Conway, H., 1977. The lubrication of a long, porous, flexible journal bearing. O'Donoghue, J., Brighton, D., Hooke, C., 1967. The effect of elastic distortions on journal bearing performance.
- Oh, K., Huebner, K., 1973. Solution of the elastohydrodynamic finite journal bearing problem.
- Orndorff, Jr., R.L., 1985. Water-lubricated rubber bearings, history and new developments. *Nav. Eng. J.* 97 (7), 39–52.
- Padovan, J., Kazempour, A., Tabaddor, F., Brockman, B., 1992. Alternative formulations of rolling contact problems. *Finite Elem. Anal. Des.* 11 (4), 275–284. [http://dx.doi.org/10.1016/0168-874X\(92\)90010-A](http://dx.doi.org/10.1016/0168-874X(92)90010-A).
- Pandey, A., Karpitschka, S., Venner, C.H., Snoeijer, J.H., 2016. Lubrication of soft viscoelastic solids. *J. Fluid Mech.* 799, 433–447.
- Persson, B.N.J., 2001. Theory of rubber friction and contact mechanics. *J. Chem. Phys.* 115 (8), 3840–3861. <http://dx.doi.org/10.1063/1.1388626>.
- Profito, F.J., Zachariadis, D.C., 2015. Partitioned fluid-structure methods applied to the solution of elastohydrodynamic conformal contacts. *Tribol. Int.* 81, 321–332.
- Profito, F., Zachariadis, D., Dini, D., 2019. Partitioned fluid-structure interaction techniques applied to the mixed-elastohydrodynamic solution of dynamically loaded connecting-rod big-end bearings. *Tribol. Int.* 140, 105767. <http://dx.doi.org/10.1016/j.triboint.2019.05.007>.
- Putignano, C., 2020. Soft lubrication: A generalized numerical methodology. *J. Mech. Phys. Solids* 134, 103748. <http://dx.doi.org/10.1016/j.jmps.2019.103748>.
- Putignano, C., 2021. Oscillating viscoelastic periodic contacts: A numerical approach. *Int. J. Mech. Sci.* 208, 106663. <http://dx.doi.org/10.1016/j.ijmecsci.2021.106663>.
- Putignano, C., Burris, D., Moore, A., Dini, D., 2021. Cartilage rehydration: The sliding-induced hydrodynamic triggering mechanism. *Acta Biomater.* 125, 90–99.
- Putignano, C., Campanale, A., 2022. Squeeze lubrication between soft solids: A numerical study. *Tribol. Int.* 176, 107824. <http://dx.doi.org/10.1016/j.triboint.2022.107824>.
- Putignano, C., Carbone, G., Dini, D., 2016. Theory of reciprocating contact for viscoelastic solids. *Phys. Rev. E* 93, 043003. <http://dx.doi.org/10.1103/PhysRevE.93.043003>.
- Putignano, C., Dini, D., 2017. Soft matter lubrication: does solid viscoelasticity matter? *ACS Appl. Mater. Interfaces* 9 (48), 42287–42295.
- Putignano, C., Menga, N., Afferrante, L., Carbone, G., 2019. Viscoelasticity induces anisotropy in contacts of rough solids. *J. Mech. Phys. Solids* 129, 147–159. <http://dx.doi.org/10.1016/j.jmps.2019.03.024>.
- Rahnejat, H., 2010. *Tribology and Dynamics of Engine and Powertrain: Fundamentals, Applications and Future Trends*. Elsevier.
- Reynolds, O., 1886. IV. On the theory of lubrication and its application to Mr. Beauchamp tower's experiments, including an experimental determination of the viscosity of olive oil. *Philos. Trans. R. Soc. Lond.* (177), 157–234.
- Rohde, S., Whicker, D., Booker, J., 1979. Elastohydrodynamic squeeze films: effects of viscoelasticity and fluctuating load.
- Santeramo, M., Putignano, C., Vorlauffer, G., Krenn, S., Carbone, G., 2023a. On the role of viscoelasticity in polymer rolling element bearings: Load distribution and hysteretic losses. *Mech. Mach. Theory* 189, 105421.
- Santeramo, M., Putignano, C., Vorlauffer, G., Krenn, S., Carbone, G., 2023b. Viscoelastic steady-state rolling contacts: A generalized boundary element formulation for conformal and non-conformal geometries. *J. Mech. Phys. Solids* 171, 105129. <http://dx.doi.org/10.1016/j.jmps.2022.105129>.
- Scaraggi, M., Persson, B., 2014. Theory of viscoelastic lubrication. *Tribol. Int.* 72, 118–130. <http://dx.doi.org/10.1016/j.triboint.2013.12.011>.
- Shukla, A., Datta, T., 1999. Optimal use of viscoelastic dampers in building frames for seismic force. *J. Struct. Eng.* 125 (4), 401–409.
- Stupkiewicz, S., Lengiewicz, J., Sadowski, P., Kucharski, S., 2016. Finite deformation effects in soft elastohydrodynamic lubrication problems. *Tribol. Int.* 93, 511–522. <http://dx.doi.org/10.1016/j.triboint.2015.03.016>, 41st Leeds-Lyon Symposium on Tribology - Integrated Tribology.
- Venner, C.H., Lubrecht, A.A., 2000. *Multi-Level Methods in Lubrication*. Elsevier.
- Vlădescu, S.-C., Putignano, C., Marx, N., Keppens, T., Reddyhoff, T., Dini, D., 2019. The percolation of liquid through a compliant seal—An experimental and theoretical study. *J. Fluids Eng.* 141 (3).
- Yousef, S., 2016. 16 - polymer nanocomposite components: A case study on gears. In: Njuguna, J. (Ed.), *Lightweight Composite Structures in Transport*. Woodhead Publishing, pp. 385–420. <http://dx.doi.org/10.1016/B978-1-78242-325-6.00016-5>.